Three-Flavor Subleading Effects and Systematic Uncertainties in Super-Kamiokande

Eligio LISI
Istituto Nazionale di Fisica Nucleare, Via Amendola 173, I-70126 Bari, Italy

Abstract

Subleading 3ν effects in atmospheric ν oscillations (including those induced by nonzero $\delta m^2 = m_2^2 - m_1^2$ at any value of θ_{13}) have been considered long ago, but only recently the Super-Kamiokande (SK) data have started to show some weak sensitivity to them, sparking an increasing theoretical and experimental interest. I discuss some selected (analytical, numerical, and statistical) topics related to such subleading effects, which might help their understanding in future atmospheric ν searches characterized by higher statistics and smaller systematics.

1. Introduction and notation

In this contribution to the Workshop (mainly based on recent work done in collaboration with G.L. Fogli, A. Marrone, A. Palazzo [1], and on earlier work with G.L. Fogli, D. Montanino [2], and G. Scioscia [3]) I briefly discuss the following issues related to subleading effects in atmospheric three-neutrino oscillations: Old phenomenological results (Sec. 2), Recent phenomenological results (Sec. 3), Analytical expectations (Sec. 4), Numerical examples (Sec. 5), Systematic uncertainties (Sec. 6). Hereafter, for simplicity, the mixing matrix U is taken real, i.e., the CP violating phase δ is assumed to be either 0 or π:

$$U_{\rm CP} = \begin{pmatrix} c_{13}c_{12} & s_{12}c_{13} & \pm s_{13} \\ -s_{12}c_{23} \mp s_{23}s_{13}c_{12} & c_{23}c_{12} \mp s_{23}s_{13}s_{12} & s_{23}c_{13} \\ s_{23}s_{12} \mp s_{13}c_{23}c_{12} & -s_{23}c_{12} \mp s_{13}s_{12}c_{23} & c_{23}c_{13} \end{pmatrix} , \qquad (1)$$

where the upper (lower) sign refers to $\delta = 0$ ($\delta = \pi$). The two cases are formally related by the replacement $s_{13} \to -s_{13}$. Here, $s_{ij} = \sin\theta_{ij}$ and $c_{ij} = \cos\theta_{ij}$. Concerning the squared mass differences, the smallest one ("solar") is defined as

$$\delta m^2 = m_2^2 - m_1^2 > 0 \qquad (2)$$

while the other one ("atmospheric") is formally defined as [1]

$$\Delta m^2 = \left| m_3^2 - \frac{m_1^2 + m_2^2}{2} \right| . \qquad (3)$$

pp. 19–31

The squared mass matrix is then

$$M^2 = \frac{m_2^2 + m_1^2}{2}\,\mathbf{1} + \mathrm{diag}\left(-\frac{\delta m^2}{2}, +\frac{\delta m^2}{2}, \pm\Delta m^2\right) \,, \tag{4}$$

where the upper (lower) sign refers to normal (inverted) hierarchy [1].

Within such conventions, the parameter space for atmospheric 3ν oscillations is $(\pm\Delta m^2, \theta_{23}, \theta_{13} \,|\, \delta m^2, \theta_{12})$; however, the last two parameters are ineffective in the frequently-used limit $\delta m^2/\Delta m^2 \to 0$ (one-mass-scale dominance).

It is useful to remind that matter effects [4] are typically (but not necessarily) relevant when the term $A(x) = 2\sqrt{2}G_F N_e(x)E$ is of the same order of either Δm^2 or δm^2. Numerically, this condition corresponds to either

$$\frac{A}{\Delta m^2} \simeq 1.3 \left(\frac{2.4\times10^{-3}\ \mathrm{eV}^2}{\Delta m^2}\right)\left(\frac{E}{10\ \mathrm{GeV}}\right)\left(\frac{N_e}{2\ \mathrm{mol/cm}^3}\right) \sim O(1) \,, \tag{5}$$

which can occur in the SK samples [5] of multi-GeV, stopping muon, and τ-appearance neutrino events, or

$$\frac{A}{\delta m^2} \simeq 3.8 \left(\frac{8.0\times10^{-5}\ \mathrm{eV}^2}{\Delta m^2}\right)\left(\frac{E}{1\ \mathrm{GeV}}\right)\left(\frac{N_e}{2\ \mathrm{mol/cm}^3}\right) \sim O(1) \,, \tag{6}$$

which can occur in the SK samples of sub-GeV events and of atmospheric background to supernova relic ν, as well as in low-energy (sub-GeV) long-baseline accelerator ν events in K2K [6]. The electron density N_e is ~ 2 (~ 5) mol/cm^3 in the Earth's mantle (core). With the previous notation, notice that [1]

$$+A(x) \;\to\; -A(x) \quad \text{flips (anti)neutrinos} \,, \tag{7}$$

$$+\Delta m^2 \;\to\; -\Delta m^2 \quad \text{flips hierarchy} \,, \tag{8}$$

$$+s_{13} \;\to\; -s_{13} \quad \text{flips CP parity} \,. \tag{9}$$

2. Archeo-phenomenology

Since $\delta m^2 \ll \Delta m^2$, one can naturally separate two classes of experiments: (1) those mainly sensitive to δm^2 (solar, long-baseline reactor), and (2) those mainly sensitive to Δm^2 (atmospheric, long-baseline accelerator, short-baseline reactor). As a 0th-order approximation, one can take $\Delta m^2 = \infty$ in the first case, and $\delta m^2 = 0$ in the second case (one-dominant-mass-scale approximation).

Subleading corrections to this simplified picture (in order to account for both mass scales, δm^2 and Δm^2, at the same time) were considered long ago. E.g., one can already find in a classic review [7] both the subdominant δm^2-correction to the effective mixing angle $\tilde{\theta}_{13}$ in matter,

$$\frac{\sin 2\theta_{13}}{\sin 2\tilde{\theta}_{13}} \simeq \sqrt{\left(\frac{A}{\Delta m^2 + \frac{\delta m^2}{2}\cos 2\theta_{12}} - \cos 2\theta_{13}\right)^2 + \sin^2 2\theta_{13}} \,, \tag{10}$$

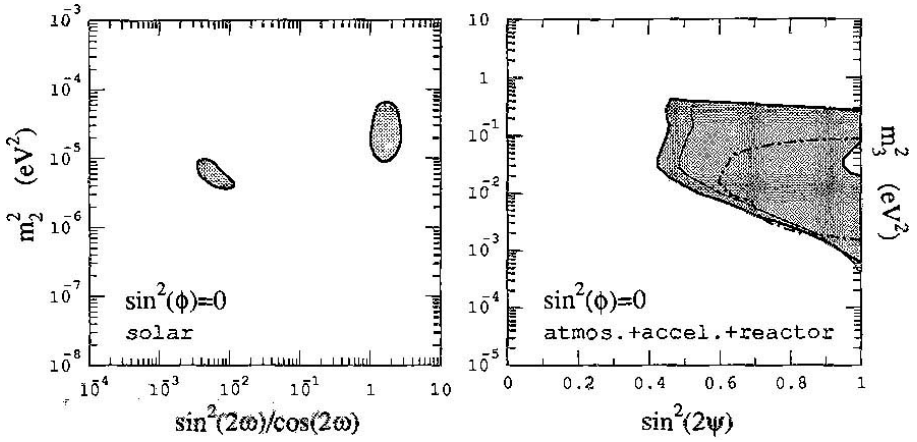

Fig 1. Results extracted (for $\theta_{13} = 0$) from an early analysis [2] of solar neutrino data (left panel) and atmospheric neutrino data plus reactor constraints (right panel), including both mass scales δm^2 and Δm^2n. Thin lines: 0th-order results in $\delta m^2/\Delta m^2$ (one-mass-scale approximation). Thick lines: Two-mass-scale results. The difference is graphically visible only for the atmospheric allowed region. Translation from old [2] to current notation: $(m_2^2, m_3^2) \to (\delta m^2, \Delta m^2)$ and $(\omega, \phi, \psi) \to (\theta_{12}, \theta_{13}, \theta_{23})$.

and the subdominant ν_3-correction to the effective mixing angle $\tilde{\theta}_{12}$ in matter,

$$\frac{\sin 2\theta_{12}}{\sin 2\tilde{\theta}_{12}} \simeq \sqrt{\left(\frac{Ac_{13}^2}{\delta m^2} - \cos 2\theta_{12}\right)^2 + \sin^2 2\theta_{12}} \ . \tag{11}$$

as well as the two-mass-scale corrections to the effective squared mass eigenvalues in matter: $\tilde{m}_i^2 = \tilde{m}_i^2(\delta m^2, \Delta m^2, \theta_{12}, \theta_{13}, A)$, valid for $A = \text{const}$ [7].

In the general case $A = A(x)$, two-mass-scale corrections must be implemented numerically; e.g., atmospheric neutrinos must be evolved through successive Earth shells with flavor-conserving conditions at the shell boundaries. An early numerical analysis of solar and atmospheric neutrino oscillation phenomenology, taking into account both scales (δm^2 and Δm^2) was presented in [2], where it was shown that the corrections to the zeroth-order approximation in the small parameter $\delta m^2/\Delta m^2$ were modest in all cases of interest, and for any value of θ_{13}. Figure 1, extracted from [2] for the particular case $\theta_{13} = 0$, shows that the difference was not graphically visible for the high-δm^2 solar neutrino solutions allowed at that time (including the currently "true" solution at large mixing angle, LMA), and produced a very modest shift towards smaller θ_{23} angles for the atmospheric neutrino allowed region. These early features appear to persist in current phenomenological analyses of up-to-date experimental data [8], as we shall see in the next section.

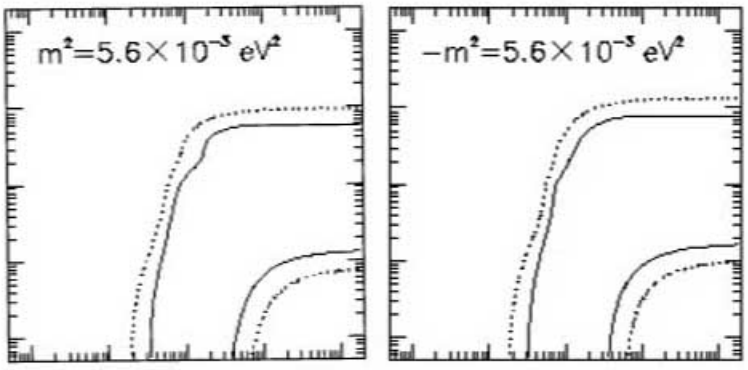

Fig 2. Results extracted (for $\Delta m^2 \equiv m^2 = 5.6 \times 10^{-3}$ eV^2) from an early one-mass-scale analysis of atmospheric neutrino data [3] with unconstrained θ_{13} in both hierarchies. The x and y axis are spanned by $\tan^2\theta_{23} \in [10^{-2}, 10^2]$ and $\tan^2\theta_{13} \in [10^{-2}, 10^2]$, respectively. The differences between the allowed regions in normal hierarchy (left panel) and inverted hierarchy (right panel) were very small.

Other interesting (and entangled) subdominant effects in atmospheric ν oscillations are induced by $\theta_{13} \neq 0$ and by our ignorance of the mass hierarchy, $\text{sign}(\pm\Delta m^2) = \pm 1$. Also such effects were considered quite early [3], and unfortunately they remain weak even with improved data and analyses (see [1] and refs. therein). Figure 2 shows the results of an old analysis of atmospheric ν data [3] at 0th order in $\delta m^2/\Delta m^2$ but for unconstrained values of θ_{13} in both hierarchies. One can see that the regions allowed at that time did not change significantly when flipping hierarchy, at any value of θ_{13}. These early features also persist with current data. Therefore, possible effects of two-mass-scales, of $\theta_{13} \neq 0$, and of ν hierarchy, definitely require new-generation experiments for their observability.

3. Current phenomenology

In recent years, the interest in two-mass-scale effects in atmospheric neutrino oscillations has been especially revived in [9, 10], where the main features of the effects have been discussed analytically, and where one can also find references to earlier numerical works. Having entered the era of precision neutrino physics, it is worthwhile to include systematically such effects which, although small, are not smaller than others one takes care of (see below). Phenomenological analyses to up-to-date SK data [8, 1] appear to show, in particular, that δm^2 effects in atmospheric neutrino oscillations tend to shift θ_{23} slightly below maximal mixing (i.e., the best-fit is at $\theta_{23} < \pi/4$), in order to account for part of the possible "electron excess" emerging in the sub-GeV SK data sample [8, 1].

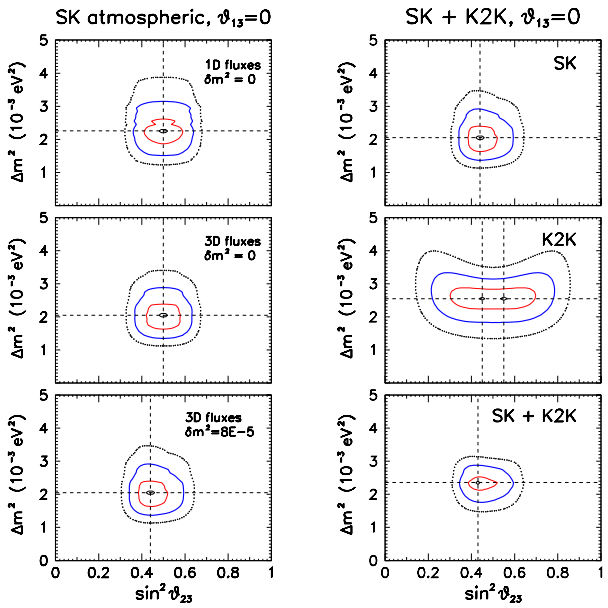

Fig 3. Regions allowed by up-to-date SK and K2K data at 1, 2, and 3 standard deviations ($\Delta\chi^2 = 1, 4, 9$) in the $(\Delta m^2, \sin^2\theta_{23})$ plane, for $\theta_{13} = 0$ (taken from [1]). Left panels: SK analysis with $\delta m^2 = 0$ and 1-dimensional (1D) atmospheric ν flux input (top), with $\delta m^2 = 0$ and 3D flux input (middle), and with $\delta m^2 = 8 \times 10^{-5}$ eV^2 and 3D input (bottom). Right panels: regions allowed separately by SK data (top) and K2K data (middle), and by the SK+K2K combination (bottom).

Figure 3 [1] (left panels) shows small effects that are now included in state-of-the-art analyses of the latest SK data [8, 1] on atmospheric neutrino events. The middle and top panels differ by the input neutrino fluxes (3D [11] instead of 1D, respectively), which shift Δm^2 by about half-standard-deviation downwards. The bottom and middle panels differ by the inclusion of $\delta m^2 = 8 \times 10^{-5}$ eV^2 from the current LMA solution to the solar neutrino problem, whose effects is to shift $\sin^2\theta_{23}$ by about half-standard-deviation downwards. Such effects are small and, unfortunately, not statistically significant; however, there is no reason to keep the first and to neglect the second: both should be taken into account in improved analyses of current data [8, 1] and prospective data [12]. Another small effect on the shape of the allowed region is provided by the inclusion of the K2K spectral data [6], which do not alter the bounds on $\sin^2\theta_{23}$ but help to strengthen the upper limit on Δm^2, as shown in the right panels of Fig. 3.

Figure 4 [1] shows that the previous results of the SK+K2K analysis at $\theta_{13} = 0$ (Fig. 3) are not significantly altered for unconstrained θ_{13} (within CHOOZ reactor constraints [13]), in all the four CP-conserving cases $[\cos\delta = \pm 1] \otimes [\mathrm{sign}(\pm\Delta m^2) = \pm 1]$; in particular, the preference for $\sin^2\theta_{23} < 1/2$ at best

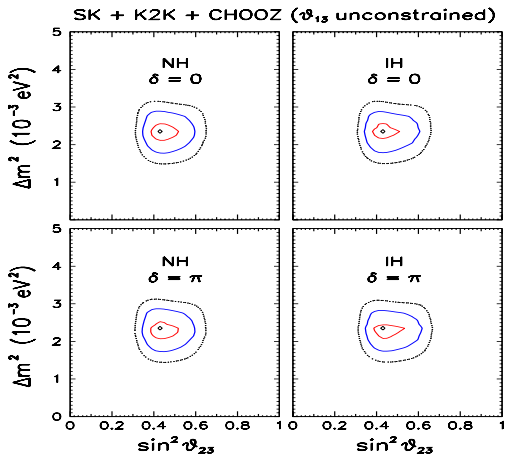

Fig 4. Three-neutrino analysis of SK+K2K+CHOOZ data, including subleading LMA effects. The results, marginalized with respect to s^2_{13}, are shown in the $(\Delta m^2, s^2_{23})$ plane for the two hierarchies (left *vs* right panels) and the two CP-conserving cases (top *vs* bottom panels). Contours refer to 1, 2, and 3 σ.

fit seems stable. However, it should be emphasized that such preference is not statistically significant, and thus it might disappear by including further experimental information. In particular, a preliminary analysis of the SK collaboration [14] including an optimized data binning and a refined treatment of systematics [14, 15] seems to find the best fit at $\sin^2\theta_{23} \simeq 1/2$. It is thus unclear if the preference for $\sin^2\theta_{23} < 1/2$ found here and in [8] will persist in the future, although the possible electron excess emerging in the current SK low-energy data seems to justify such preference [1, 8].

4. Analytical expectations

Our calculations of atmospheric ν oscillations are based on a full 3ν numerical evolution. Semianalytical approximations (although not used in the final results) can, however, be useful to understand the behavior of the oscillation probability and of some atmospheric ν observables. An important observable is the excess of expected electron events (N_e) as compared to no oscillations (N^0_e):

$$\Delta_e \equiv \frac{N_e}{N^0_e} - 1 = (P_{ee} - 1) + r\, P_{e\mu} \ , \tag{12}$$

where $P_{\alpha\beta} = P(\nu_\alpha \to \nu_\beta)$, and r is the ratio of atmospheric ν_μ and ν_e fluxes ($r \sim 2$ and ~ 3.5 at sub-GeV and multi-GeV energies, respectively). In fact, this quantity is zero when both $\theta_{13} = 0$ and $\delta m^2 = 0$, and is thus well suited to study the associated subleading effects (which may carry a dependence on the matter

density) in cases when δm^2 and θ_{13} are different from zero [9]. In the simplified case $A = \text{const}$, and using the approximations for the mass-mixing parameters in matter reported in [7], we get [1] that the electron excess at sub- or multi-GeV energies can be written as a sum of three terms,

$$\Delta_e \simeq \Delta_1 + \Delta_2 + \Delta_3 \ , \tag{13}$$

$$\Delta_1 \simeq \sin^2 2\tilde{\theta}_{13} \sin^2 \left(\Delta m^2 \frac{\sin 2\theta_{13}}{\sin 2\tilde{\theta}_{13}} \frac{L}{4E} \right) \cdot (r s_{23}^2 - 1) \tag{14}$$

$$\Delta_2 \simeq \sin^2 2\tilde{\theta}_{12} \sin^2 \left(\delta m^2 \frac{\sin 2\theta_{12}}{\sin 2\tilde{\theta}_{12}} \frac{L}{4E} \right) \cdot (r c_{23}^2 - 1) \tag{15}$$

$$\Delta_3 \simeq \sin^2 2\tilde{\theta}_{12} \sin^2 \left(\delta m^2 \frac{\sin 2\theta_{12}}{\sin 2\tilde{\theta}_{12}} \frac{L}{4E} \right) \cdot r s_{13} c_{13}^2 \sin 2\theta_{23} (\tan 2\tilde{\theta}_{12})^{-1} \ , \tag{16}$$

with $\tilde{\theta}_{13}$ and $\tilde{\theta}_{12}$ defined in Eqs. (10) and (11).

The above expressions for Δ_i, which hold for neutrinos with normal hierarchy and $\delta = 0$, coincide with those reported in [9] (up to higher-order terms or CP-violating terms, not included here). The corresponding expressions for antineutrinos, for inverted hierarchy, and for $\delta = \pi$, can be obtained through the replacements in Eqs. (7), (8), and (9), respectively. Under such transformations: (1) all Δ_i's are affected by $A \to -A$ through $\tilde{\theta}_{12}$ or $\tilde{\theta}_{13}$; (2) only Δ_1 is sensitive to $\Delta m^2 \to -\Delta m^2$; (3) only Δ_3 is sensitive to $+s_{13} \to -s_{13}$.

Concerning the dependence on the oscillation parameters, one has that: (1) all Δ_i's depend on θ_{23}; (2) Δ_1 arises for $\theta_{13} > 0$, and is independent of δm^2; (3) Δ_2 arises for $\delta m^2 > 0$, and is independent of θ_{13}; only Δ_3 ("interference term" [9]) depends on both θ_{13} and δm^2.

Concerning the dependence on energy, in the sub-GeV range one has that: (1) $\tilde{\theta}_{13} \simeq \theta_{13}$, so that for large L the first term is simply $\Delta_1 \simeq 2 s_{13}^2 c_{13}^2 (r s_{23}^2 - 1)$; (2) since $r \simeq 2$, the term Δ_1 flips sign as s_{23}^2 crosses the maximal mixing value $1/2$ [16], and similarly for Δ_2 (with opposite sign) [9]; (3) for neutrinos, which give the largest contribution to atmospheric events, it turns out that $\tan 2\tilde{\theta}_{12} < 0$, and thus typically $\Delta_3 < 0$ for $\delta = 0$ ($\Delta_3 > 0$ for $\delta = \pi$). In the multi-GeV range one has that $\tilde{\theta}_{12} \simeq \pi/2$, so that only Δ_1 dominates, with typically positive values (being $r \simeq 3.5$ and s_{23}^2 not too different from $1/2$).

5. Numerical examples

Figure 5 shows exact numerical examples (extracted from our SK data analysis [1]) where, from top to bottom, the dominant term is Δ_1, Δ_2, and Δ_3. The dashed histograms represent theoretical predictions R_n in each zenith bin

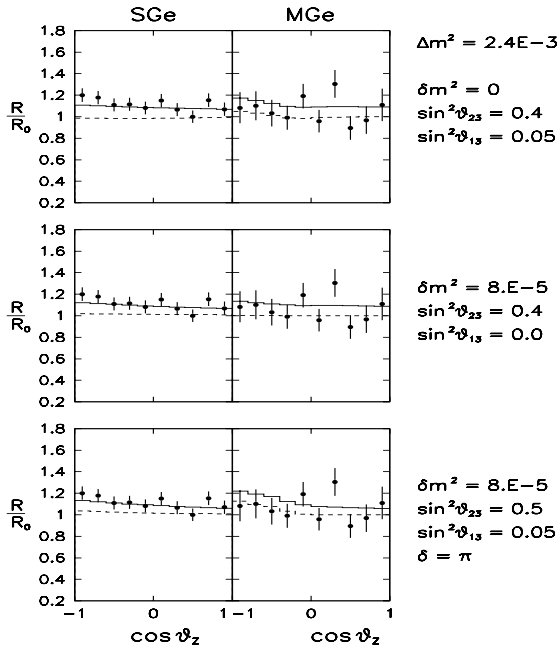

Fig 5. Representative examples of subleading 3ν effects in the sub-GeV and multi-GeV electron samples (SGe and MGe), as a function of the cosine of the lepton zenith angle θ_Z, normalized to no-oscillation expectations in each bin. See also [1].

while the solid histograms represent the predictions $\overline{R}_n$ shifted through independent systematic uncertainties c_{nk},

$$R_n \to \overline{R}_n = R_n + \sum_k \xi_k \, c_{nk} \ , \tag{17}$$

whose amplitudes ξ_k are constrained through a quadratic penalty term, within the so-called pull approach to the χ^2 analysis [17]. Both unshifted and shifted predictions are normalized to no-oscillation expectations R_n^0 in each bin. Let us focus on the dashed histograms in Fig. 5, where we have taken $\Delta m^2 = +2.4 \times$ $\times 10^{-3}$ eV^2 (normal hierarchy); other relevant parameters are indicated at the right of each panel. In the upper panel, we have set $\delta m^2 = 0$, so as to switch off Δ_2 and Δ_3. We have also taken $s^2_{23} = 0.4 < 0.5$, so that $\Delta_1 < 0$ in the sub-GeV sample; it is instead $\Delta_1 > 0$ in the multi-GeV sample. In the middle panel, we have set $(\delta m^2, \sin^2\theta_{12})$ at their best-fit LMA values, but have taken $\sin^2\theta_{13} = 0$, so that only Δ_2 survives. In particular, while there is no observable effect of Δ_2 in the multi-GeV sample (where the energy is relatively high and $\sin 2\tilde{\theta}_{12} \simeq 0$), the effect is positive for sub-GeV neutrinos, where $s^2_{23} = 0.4 < 1/2$. Notice that the upper and middle panel results are insensitive to $\delta = 0$ or π, since $\Delta_3 \simeq 0$ in both cases. Finally, in the bottom plot we have taken $s^2_{23} = 1/2$, so as to suppress

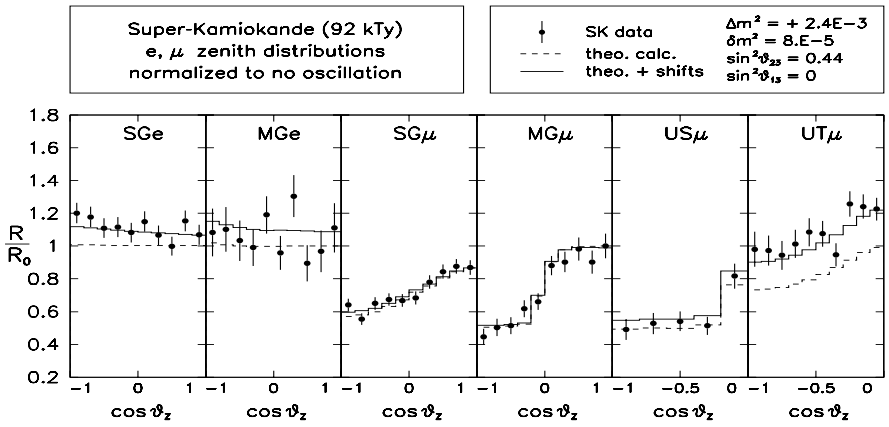

Fig 6. SK data and predictions for sub-GeV electrons (SGe), multi-GeV electrons (MGe), sub-GeV muons (SGμ), multi-GeV muons (MGμ), upward stopping muons (UPμ), upward through-going muons (UTμ). Data are shown by dots with $\pm 1\sigma$ statistical error bars. The histograms represent our calculations at the SK+K2K best fit in Fig. 3 (dashed: no systematic shifts; solid: systematic shifts allowed).

Δ_1 and Δ_2 is the sub-GeV sample, where $\Delta_3 > 0$ for our choice $\delta = \pi$. In the multi-GeV sample, however, Δ_1 is still operative.

The subleading dependence of atmospheric ν_e events on the hierarchy, δm^2, θ_{13}, and CP-parity is intriguing and is thus attracting increasing interest. However, Fig. 5 clearly shows that such dependence is currently well hidden, not only by statistical uncertainties (vertical error bars) but, more dangerously, by allowed systematic shifts of the theoretical predictions (solid histograms). For instance, in the upper panel, systematics can "undo" the negative effect of Δ_1 in the SGe sample and make it appear positive. In all cases, they tend to magnify the zenith spectrum distortion; this is particularly evident in the right middle panel, where the unshifted theoretical prediction is flat.

Figure 6 shows the importance of systematics in SK from a global viewpoint. The difference between shifted and unshifted predictions is significant, and even larger than the statistical errors, in seemingly unrelated samples: SG+MG electrons, and upward through-going (UT) muons. In the latter sample, upward systematics shifts are strictly needed, since the unshifted predictions are definitely too low with respect to the data; i.e., since we cannot invoke ν_μ oscillation "appearance" to explain the UTμ "excess," we conclude that it must be due to systematics. With the same logic, we cannot exclude that the SGe and MGe "excess" may also be generated by systematics, rather than by the 3ν effects we are looking for. Therefore, caution is needed in interpreting any (weak) indication of 3ν effect in current SK data, including the slight preference for non-maximal θ_{23}.

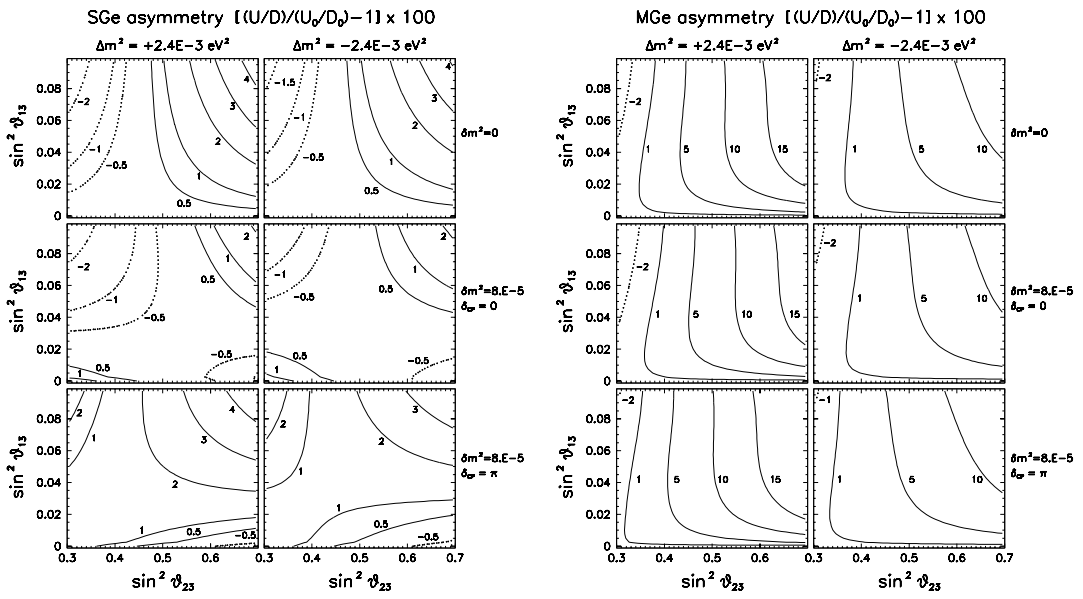

Fig 7. Isolines of the up-down electron asymmetry in the SG and MG samples, normalized to no-oscillation expectations. See the text and Ref. [1] for details.

We think it useful to quantify at which level one has to reduce systematic uncertainties, in order to appreciate subleading effects in future, larger SK-like atmospheric neutrino experiments such as those proposed in [18, 19, 20]. Since normalization systematics are large (as evident from Fig. 6), we prefer to focus on a normalization-independent quantity, namely, the fractional deviation of the up-down asymmetry of electron events from their no-oscillation value,

$$A_e = \frac{U/D}{U_0/D_0} - 1 \ , \tag{18}$$

where "up" (U) and "down" (D) refer to the zenith angle ranges $\cos\theta_z \in [-1, -0.4]$ and $[0.4, 1]$, respectively. We perform a full numerical calculation of this quantity for both SGe and MGe events, assuming the SK experimental setting for definiteness. Notice that the up-down asymmetry involves the first and last three bins of the SGe and MGe samples in Fig. 6.

Fig. 7 shows isolines of $100 \times A_e$ for the SGe sample (left) and MGe sample (right) plotted in the $(\sin^2\theta_{23}, \sin^2\theta_{13})$ plane at fixed $\Delta m^2 = 2.4 \times 10^{-3}$ eV^2, for both normal hierarchy ($+\Delta m^2$, left panels) and inverse hierarchy ($-\Delta m^2$, right panels). In both hierarchies, we consider first the "academic" case $\delta m^2 = 0$ (top panels), then we switch on the LMA parameters $(\delta m^2, \sin^2\theta_{12})$ at their best-fit values, for the the two CP-conserving cases $\delta = 0$ (middle panels) and $\delta = \pi$ (bottom panels). A thorough discussion of the behavior of the A_e isolines can be

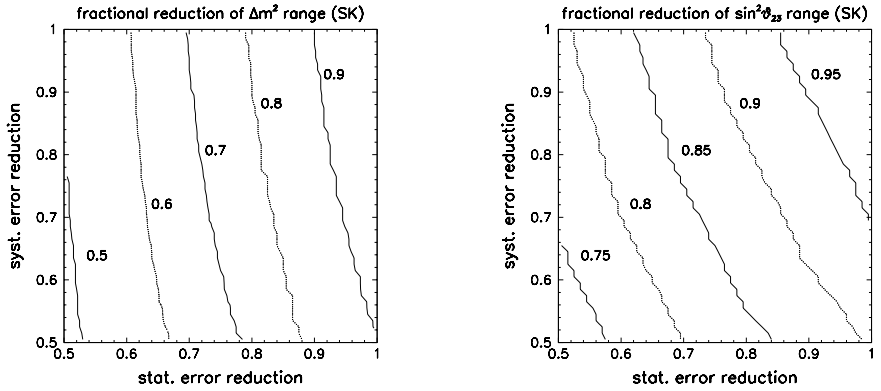

Fig 8. Isolines of the fractional reduction of the ($\pm 2\sigma$) SK allowed range for Δm^2 (left) and for $\sin^2\theta_{23}$ (right), as a function of hypothetical fractional reduction of all statistical errors (x-axis) and of all systematic errors (y-axis).

found in [1]. Here we only emphasize that: (1) in the SGe case, the asymmetry is typically at the percent or sub-percent level for $\sin^2\theta_{13} <$ few%; therefore, statistical and systematic uncertainties need to be reduced at this extraordinary small level in order to really "observe" the effects in future atmospheric neutrino experiments; (2) The MGe asymmetry can be of $O(10\%)$ and thus relatively large; with some luck, such asymmetry might be seen in future large Cherenkov detectors if θ_{13} is not too small. In all cases, systematics need drastic reduction. Dedicated studies are needed [14, 15] to understand which systematic sources (atmospheric flux, hadronic and leptonic cross section, detector, data analysis) are most dangerous for the detection of 3ν effects.

6. Is SK limited by systematics?

Dedicated studies of systematic error reduction can also be motivated by observing that the role of systematics can be counter-intuitive. For instance, since statistical and systematic errors in Fig. 6 are comparable, one could guess that the $(\Delta m^2, \sin^2\theta_{23})$ parameter estimation would equally benefit from a reduction of statistical and systematic errors. However, we have performed numerical experiments which show that, formally, it is more important to reduce statistical errors. In particular, Fig. 8 shows the fractional reduction of the SK allowed range for Δm^2 (left) and $\sin^2\theta_{23}$ (right), when either statistical or systematic errors are reduced by an overall factor between 1 (current errors) and 0.5 (halved errors). It can be seen that the parameter estimates (especially for Δm^2) improve faster by reducing statistical rather than systematic errors. Similar results have been obtained in [21]. Thus, one might think that SK is not limited by systematics.

However, this counter-intuitive conclusion might be premature, since it assumes that we perfectly know all sources of systematics. In terms of the pull method [Eq. (17)], this means that we are assuming perfect knowledge of all c_{nk}'s, i.e., of the "response" of any predictions R_n to any systematic source ξ_k. This assumption might be too optimistic. The response is never known with infinite precision, and the c_{nk} have their own uncertainties ("errors of the errors"). For instance, the response of the zenith distributions in Figs. 5 and 6 to up-down detector systematics is typically assumed to be linear in $\cos\theta_Z$, but this is just an empirical assumption: a tolerance for (currently neglected) non-linearities in the detector response could be envisaged. Although such "second-order" systematic error sources are not crucial at present, they might become so in the future, if one really aims at reaching a (sub)percent level for systematic uncertainties, in order to detect small 3ν effects in atmospheric neutrino experiments.

The statistical techniques needed to deal with the c_{nk} uncertainties (the "errors of the errors") are still to be envisaged; perhaps this task will require detailed and massive numerical experiments (i.e., Monte-Carlo simulations of small variations in the c_{nk} response functions). These subtle points should be kept in mind when considering the (perhaps optimistic) results of some prospective studies, where the currently known SK systematics are simply reduced by an arbitrary factor, with no variation or uncertainty assumed for the c_{nk}'s.

7. Conclusions

Subleading three-flavor effects in atmospheric neutrinos have been studied for a long time and in different phenomenological aspects. Now we know that solar neutrinos oscillations are driven by $\delta m^2 \simeq 8 \times 10^{-5}$ eV^2, and thus some δm^2-induced 3ν effects must be also present in atmospheric neutrino oscillations (dominated by $\Delta m^2 \sim 2.4 \times 10^{-3}$ eV^2).

Currently, it seems that δm^2-induced effects help to fit the electron excess slightly better (especially in the sub-GeV sample) for non-maximal θ_{23}. But the statistical significance of this shift from maximality is small, and is not supported by the SK own analysis. The δm^2 effects are also entangled, in general, with other 3ν effects (related to θ_{13}, hierarchy, CP parity).

In both the sub- and multi-GeV samples (and especially in the former), observation of subleading 3ν effects require drastic error reduction. Reduction of statistical errors calls for larger detectors; reduction of systematics (on fluxes, cross-sections, detector) demands dedicated studies, and perhaps new statistical techniques to deal with subtle effects. The task is challenging, but the observation of 3ν effects in atmospheric ν experiments would be extremely rewarding.

Acknowledgments

The author is grateful to T. Kajita and to all the organizers of this stimulating workshop for kind hospitality. This work is supported by the Italian Ministero dell'Istruzione, Università e Ricerca (MIUR) and Istituto Nazionale di Fisica Nucleare (INFN) through the "Astroparticle Physics" research project.

References

[1] G.L. Fogli, E. Lisi, A. MArrone, and A. Palazzo, hep-ph/0506083, to appear in Progress in Particle and Nuclear Physics.
[2] G. L. Fogli, E. Lisi and D. Montanino, Astropart. Phys. **4**, 177 (1995).
[3] G. L. Fogli, E. Lisi, D. Montanino and G. Scioscia, PRD **55**, 4385 (1997).
[4] L. Wolfenstein, Phys. Rev. D **17**, 2369 (1978); S. P. Mikheev and A. Yu. Smirnov, Yad. Fiz. **42**, 1441 (1985) [Sov. J. Nucl. Phys. **42**, 913 (1985)].
[5] Super-Kamiokande Collaboration, Y. Ashie *et al.*, hep-ex/0501064.
[6] K2K Collaboration, E. Aliu *et al.*, Phys. Rev. Lett. **94**, 081802 (2005).
[7] T. K. Kuo and J. T. Pantaleone, Rev. Mod. Phys. **61**, 937 (1989).
[8] M. C. Gonzalez-Garcia, M. Maltoni and A. Y. Smirnov, Phys. Rev. D **70**, 093005 (2004). See also M.C. Gonzalez-Garcia, these Proceedings.
[9] O. L. G. Peres and A. Y. Smirnov, Phys. Lett. B **456**, 204 (1999); O. L. G. Peres and A. Y. Smirnov, Nucl. Phys. B **680**, 479 (2004).
[10] M. C. Gonzalez-Garcia and M. Maltoni, Eur. Phys. J. C **26**, 417 (2003).
[11] M. Honda, T. Kajita, K. Kasahara and S. Midorikawa, Phys. Rev. D **70**, 043008 (2004). See also the website www.icrr.u-tokyo.ac.jp/~mhonda.
[12] P. Huber, M. Maltoni, and T. Schwetz, Phys. Rev. D **71**, 053006 (2005).
[13] CHOOZ Collaboration, M. Apollonio *et al.*, Eur. Phys. J. C **27**, 331 (2003).
[14] K. Okumura, these Proceedings.
[15] S. Nakayama, these Proceedings.
[16] E. Akhmedov, A. Dighe, P. Lipari and A. Smirnov, NPB **542**, 3 (1999).
[17] G. L. Fogli, E. Lisi, A. Marrone and D. Montanino, PRD **67**, 093006 (2003).
[18] UNO proposal, C.K. Jung, hep-ex/0005046.
[19] Hyper-Kamiokande: K. Nakamura, Int. J. Mod. Phys. A **18**, 4053 (2003).
[20] MEMPHYS proposal, see L. Mosca, talk at the Villars CERN/SPSC Meeting (Villars, Switzerland, 2004), available at nuspp.in2p3.fr/Frejus.
[21] S. Moriyama, in the Proceedings of *NOW 2004*, International Neutrino Oscillation Workshop (Conca Specchiulla, Otranto, 2004), edited by P. Bernardini, G.L. Fogli, and E. Lisi, Nucl. Phys. B (Proc. Suppl.) **145**.